

RESEARCH ARTICLE

Shifts in methanogenic archaea communities and methane dynamics along a subtropical estuarine land use gradient

Sebastian Euler^{1*}, Luke C. Jeffrey¹, Damien T. Maher^{1,2}, Derek Mackenzie¹, Douglas R. Tait¹

1 SCU GeoScience, Southern Cross University, Lismore, NSW, Australia, **2** School of Environment, Science and Engineering, Southern Cross University, Lismore, NSW, Australia

* euler.sebastian@gmail.com, s.euler.10@student.scu.edu.au



OPEN ACCESS

Citation: Euler S, Jeffrey LC, Maher DT, Mackenzie D, Tait DR (2020) Shifts in methanogenic archaea communities and methane dynamics along a subtropical estuarine land use gradient. PLoS ONE 15(11): e0242339. <https://doi.org/10.1371/journal.pone.0242339>

Editor: Ute Risse-Buhl, Helmholtz-Zentrum für Umweltforschung UFZ, GERMANY

Received: March 31, 2020

Accepted: October 30, 2020

Published: November 24, 2020

Peer Review History: PLOS recognizes the benefits of transparency in the peer review process; therefore, we enable the publication of all of the content of peer review and author responses alongside final, published articles. The editorial history of this article is available here: <https://doi.org/10.1371/journal.pone.0242339>

Copyright: © 2020 Euler et al. This is an open access article distributed under the terms of the [Creative Commons Attribution License](https://creativecommons.org/licenses/by/4.0/), which permits unrestricted use, distribution, and reproduction in any medium, provided the original author and source are credited.

Data Availability Statement: Environmental and microbial data used in the plots presented are available in the attached files (.csv format). Raw sequencing data are available from the Knowledge

Abstract

In coastal aquatic ecosystems, prokaryotic communities play an important role in regulating the cycling of nutrients and greenhouse gases. In the coastal zone, estuaries are complex and delicately balanced systems containing a multitude of specific ecological niches for resident microbes. Anthropogenic influences (i.e. urban, industrial and agricultural land uses) along the estuarine continuum can invoke physical and biochemical changes that impact these niches. In this study, we investigate the relative abundance of methanogenic archaea and other prokaryotic communities, distributed along a land use gradient in the subtropical Burnett River Estuary, situated within the Great Barrier Reef catchment, Australia. Microbiological assemblages were compared to physicochemical, nutrient and greenhouse gas distributions in both pore and surface water. Pore water samples from within the most urbanised site showed a high relative abundance of methanogenic *Euryarchaeota* (7.8% of all detected prokaryotes), which coincided with elevated methane concentrations in the water column, ranging from 0.51 to 0.68 μM at the urban and sewage treatment plant (STP) sites, respectively. These sites also featured elevated dissolved organic carbon (DOC) concentrations (0.66 to 1.16 mM), potentially fuelling methanogenesis. At the upstream freshwater site, both methane and DOC concentrations were considerably higher (2.68 μM and 1.8 mM respectively) than at the estuarine sites (0.02 to 0.66 μM and 0.39 to 1.16 mM respectively) and corresponded to the highest relative abundance of methanotrophic bacteria. The proportion of sulfate reducing bacteria in the prokaryotic community was elevated within the urban and STP sites (relative abundances of 8.0%–10.5%), consistent with electron acceptors with higher redox potentials (e.g. O_2 , NO_3^-) being scarce. Overall, this study showed that ecological niches in anthropogenically altered environments appear to give an advantage to specialized prokaryotes invoking a potential change in the thermodynamic landscape of the ecosystem and in turn facilitating the generation of methane—a potent greenhouse gas.

Network for Biocomplexity (doi:10.5063/F1SQ8XSB).

Funding: SE RGRG1900022 Great Barrier Reef Marine Park Authority gbrmpa.gov.au The funders had no role in study design, data collection and analysis, decision to publish, or preparation of the manuscript. DT DE180100535 Australian Research Council arc.gov.au The funders had no role in study design, data collection and analysis, decision to publish, or preparation of the manuscript.

Competing interests: The authors have declared that no competing interests exist.

1 Introduction

Land use is rapidly changing coastal environments with estuaries now representing one of the most altered and vulnerable ecosystems on the planet [1]. Estuaries are biogeochemical hotspots for carbon and nutrient cycling with nutrient inputs from a range of sources including terrestrial, riverine and groundwater [2, 3]. These nutrients are predominantly processed by bacteria and archaea within the sediments and water column of ecosystems, which can release atmospheric greenhouse gases (GHG's) such as carbon dioxide (CO₂) and methane (CH₄) [4–6]. High loading rates of organic carbon and other nutrients in areas affected by urban or agricultural land use can potentially increase emission of GHG's, compared to their pristine counterparts [7, 8].

Estuaries contribute between 1 and 7 Tg of CH₄ and 0.1 to 0.25 Gt of CO₂ to the atmosphere each year [9], with the global flux of CO₂ to the atmosphere from estuaries comparable to the uptake of the entire continental shelf, despite estuaries representing only 5% of the continental shelf equivalent surface area [10]. Increasing inputs of anthropogenic pollutants stemming from urban, industrial and agricultural runoff into adjacent estuarine ecosystems have been reported to elevate GHG fluxes [11–13]. CH₄ emissions originating from microbial sources have been suggested to contribute about 70% of all global methane emissions [14–16]. Due to the dynamic nature and spatial heterogeneity of estuarine GHG's, the underlying drivers, mechanisms and direct comparisons to microbiomes remain poorly understood [17].

Prokaryotic communities in estuaries can be complex and primarily consist of unculturable lineages, which makes laboratory-based research challenging [6, 18, 19]. Natural and anthropogenic gradients in estuarine ecosystems can be an ideal environment for gauging the response of microbes to environmental variability [20, 21]. Links between microbial communities and basic physicochemical parameters such as salinity and dissolved oxygen (DO) have been previously demonstrated in estuarine environments [21–23]. For example, Hong et al. [22] studied microbial communities in a subterranean estuary of Gloucester Beach, United States and found that the shift in microbial community compositions was mainly driven by variations in physicochemical parameters (DO, salinity, temperature). However, comprehensive investigations to further our understanding of microbial ecology and how it drives nutrient and GHG cycling under land use change are required [21, 24].

Archaeal diversity and abundance is underexplored in coastal ecosystems and plays an important role in the dynamics of GHG's and especially CH₄ production [25–27]. Methanogenic archaea are able to convert H₂, acetate, CO₂ and other carbon compounds (e.g. CO, formate, methanol, methylamines) into CH₄ [25, 28, 29]. Dissolved organic carbon (DOC) can be broken down microbially via hydrolysis, acidogenesis and acetogenesis prior to methanogenesis [30, 31]. Thermodynamically, methanogenesis is associated with a small free energy change, allowing for the synthesis between 1 (for acetoclastic methanogenesis) and 2 ATP under standard conditions, and less than 1 ATP under most environmental conditions [14, 29]. Methanogens inhabit a unique ecological niche and are highly adapted for thermodynamic energy conservation [29, 32]. Within the estuarine continuum, they likely reside and produce CH₄ in impacted locations characterized by high loads of DOC and a thermodynamic landscape that is unfavourable to many other microbes.

To gauge the factors contributing to the proliferation of specific prokaryotes occupying estuarine ecological niches, the competition between different functional groups plays an important role [33, 34]. For example, methanogens are readily outcompeted by microbial taxa utilizing more thermodynamically favourable electron acceptors such as oxygen, nitrate, iron and sulfate [35–37]. Denitrification has been shown to diminish methanogenesis via denitrifiers directly outcompeting methanogenic archaea [35, 38, 39]. Sulfate reducing bacteria do not always impact methanogen abundance and may only outcompete the latter for H₂ and acetate,

but not for labile DOC compounds like methylamines [39–41]. Recent studies have shown syntrophic interactions between methanogens and sulfate reducers co-existing in the same environment [34, 42]. This cross-feeding, however, can be accompanied by elevated GHG emissions from heavily modified coastal ecosystems [5].

A proportion of the CH₄ produced through methanogenesis can be offset by methanotrophic bacteria. Methanotrophs are divided into phylogenetically distinct types. The proteobacterial type I (*Methylococcales* order) and type II (*Methylocystaceae* family) methanotrophs are both able to use CH₄ as their sole carbon and energy source [43, 44]. Additionally, new kinds of acidophilic methanotrophs have recently been discovered within the *Verrucomicrobia* phylum (the *Methylacidiphilales* order) [45]. When not oxidized by methanotrophs, CH₄ can escape into the atmosphere [43]. Therefore, understanding the balance between methanogenesis and methanotrophy is important in constraining CH₄ emissions from impacted coastal ecosystems.

In this study we investigate the phylogenetic prevalence of CH₄ producing archaea relative to other relevant prokaryotic communities within the surface and pore water of a subtropical estuarine land use gradient (Burnett River, Australia). We correlate these microbiological assemblages with in-depth biogeochemical characterisations including physicochemical parameters (DO, salinity, temperature), nutrient availability (DOC, ammonium, nitrate and sulfate) and the GHG's CH₄ and CO₂. This multi-parameter and multi-disciplinary approach is then used to determine the influence of different land uses along the estuarine continuum on microbial and abiotic factors.

2 Materials and methods

2.1 Study site

The Burnett River estuary, situated in the subtropical Great Barrier Reef (GBR) catchment area, features a multitude of different ecological and land use zones along its length, before discharging into the Coral Sea on Australia's east coast (Fig 1). Situated adjacent to the Great Dividing Range, the region features an elevated topography with floodplain areas adjacent to the river (e.g. around Bundaberg). The subtropical climate receives a mean annual rainfall of ~1000 mm (www.bom.gov.au) with approximately one third of the rainfall occurring in summer between January and February. The average annual temperature in the region is 21.5°C with a mean maximum of 26.8°C and a mean minimum of 16.4°C. Anthropogenic development in the Burnett River estuary catchment includes widespread agricultural land use including livestock grazing and horticulture (predominantly sugarcane), as well as mining and urban development [46, 47]. A total of ~2,800,000 ha or 74% of the Burnett Catchment area is used by agriculture, with grazing accounting for ~80% of agricultural land use, while urban development (mainly the city of Bundaberg) accounts for ~13%.

The estuary mouth (Site 1) is mostly pristine, with the Barubbra Island Regional Park spanning the entire northern shore and low-density dwellings situated on the southern bank (Fig 1). Upstream from the mouth, land use is predominantly agricultural with livestock grazing and horticulture on both sides of the river (Site 2). About 13 km upstream (Site 3), the city of Bundaberg supports a population of ~70,000 (or 232 people per km²) with significant urban and industrial development (predominantly sugar industry related, e.g. distilling and cane harvester manufacturing) around the estuary. Mangroves line parts of the lower estuary channel which is bordered by agricultural and urban land uses (Sites 2, 3 & 4). Situated at the upper city boundary (Site 4), a sewage treatment plant (STP) discharges treated wastewater into the main channel. Approximately 25 km from the ocean, a concrete weir (Site 5—downstream and Site 6—upstream) moderates the tidal limit of the estuary. The weir causes a steep salinity

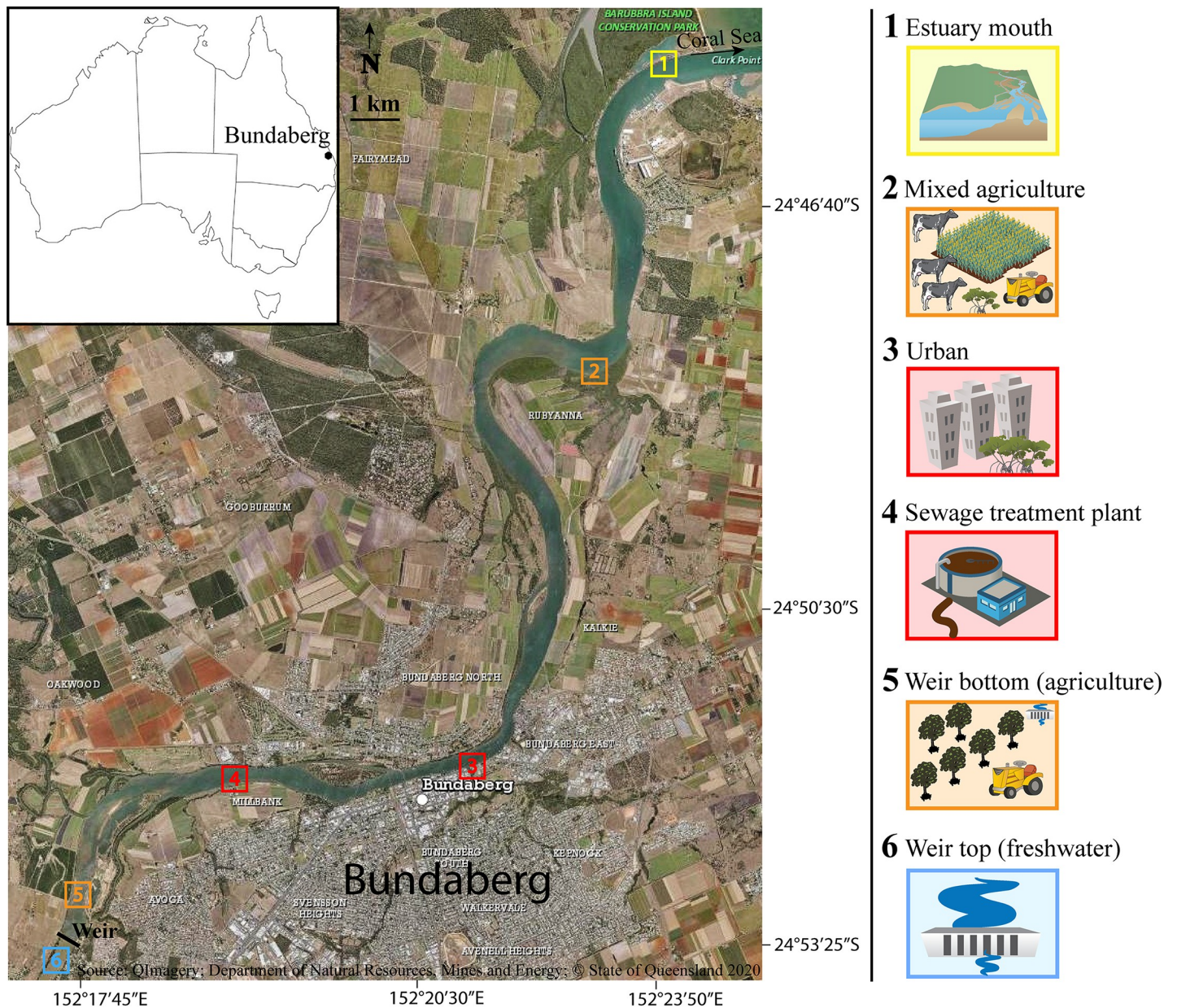


Fig 1. Map of the subtropical Burnett River estuary, situated in the GBR catchment area (Queensland, Australia), depicting study sites along the land use gradient. 1) Mouth of the estuary, mostly pristine environment; 2) Mixed agriculture site, sugar cane farming and livestock grazing; 3) Urban site within the city of Bundaberg, housing and industry; 4) Sewage treatment plant (STP), urban waste; 5) Bottom of the weir, macadamia farming; 6) Top of the weir, freshwater site.

<https://doi.org/10.1371/journal.pone.0242339.g001>

drop during dry conditions due to the separation of estuarine brackish waters and upstream fresh water inputs. Small scale horticulture (predominantly macadamia farms) is situated to the west of the weir. Above and beyond the weir are low intensity agriculture and residential developments.

2.2 Sample collection

Sampling was undertaken between the 7th and 12th of January 2019 coinciding with the end of the dry season in the region. Most of the spatial sampling was conducted from a small boat

over three consecutive days on an ebbing tide, starting at the mouth at high tide. Discrete samples for microbiological analysis and nutrient analysis were taken at each site in conjunction with continuous water column measurement of GHG's and physicochemical parameters. Surface water GHG concentrations were sampled *in situ* using a closed-loop system, where a surface water fed air-water equilibrator was connected to a Cavity Ring-Down Spectrometer (CRDS, Picarro Gas Scouter) similar to that described by Maher et al. [48]. Due to restricted boat accessibility at Sites 5 and 6, discrete surface water samples were collected from the upstream sites and stored in gas-tight 6 L bottles leaving a headspace. Physicochemical parameters were also measured continuously *in situ* using a submersible multi-parameter sonde (YSI Exo2) measuring DO (% Sat), pH, salinity and temperature (°C).

At each site, discrete surface water samples (~5 cm depth) were taken from the estuary, as well as shallow groundwater / pore water samples (80–100 cm depth) from the immediate adjacent shoreline (within 5 meters). Shallow groundwater wells were excavated in the intertidal zone, with each well purged dry three times to ensure fresh pore water was collected. Wells were left to recharge in between sampling rounds. With this method, the signal was integrated over the whole depth range. There was little change in water table depth along the estuary and sampling sites. For both surface water and pore water samples, DOC samples were filtered with 0.7 µm glass microfiber filters and stored in 40 ml borosilicate vials amended with saturated H₃PO₄ to stop further microbial processing. Ammonium, nitrate and sulfate samples were filtered using 0.45 µm cellulose acetate filters and stored in 10 ml polycarbonate vials (Thomas Scientific).

At all sites, individual microbial samples of both surface waters and pore waters were extracted by hand using fresh sterile examination gloves, filters and syringes to avoid cross-contamination. Microbial samples were filtered with 0.22 µm membrane filters (Isopore) and stored in sterile 1.5 ml polycarbonate vials (Eppendorf) pre-filled with DNAGard (Sigma) in a flow hood maintaining sterile conditions. As water was filtered until the membrane filters' capacity was saturated to maximize the yield of microbial tissue, total sample volumes varied from 41 ml to 129 ml for pore water samples and from 152 ml to 420 ml for surface water samples. In order to gather duplicates, sampling took place within 2 minutes of each other at each site in the same area (~1 m diameter), with the exception of Site 1 surface water samples, where the sampling vessel drifted due to tidal current and the duplicate had to be discarded. Hierarchical clustering was carried out with GENE-E (Broad Institute, MIT) using negative Pearson correlation metrics which indicated low dissimilarity between microbiological sample duplicates (S1 Fig).

2.3 Environmental sample analysis

DOC concentrations were determined using a total organic carbon analyser coupled with an isotope ratio mass spectrometer (Thermo Fisher Delta-V Plus) and a continuous flow system (Thermo Fisher ConFlo) with a precision of 0.02 mM [49]. Ammonium and nitrate concentrations were measured via flow injection analysis (Lachat 8500), with an analytical error of 5.1% for NH₄⁺ and 6.2% for NO₃⁻ [50]. Sulfate concentrations were determined via ion chromatography (Metrosep A Supp4–250 column and Metrosep RP2 guard column; eluent contained 2 mM NaHCO₃, 2.4 mM Na₂CO₃ and 5% acetone) with an analytical error of ~2% [51]. For discrete GHG samples, the gas-tight 6 L bottles were connected into a closed loop with the CRDS, with an inlet tubing bubbler used to encourage headspace equilibration. Each water sample was run for ≥ 2 h or until gas concentrations between the water sample and headspace equilibrated. GHG and nutrient concentrations were averaged for each sampling location and error propagation for measurement uncertainties applied.

2.4 Microbiological sample analysis

DNA from microbial samples was isolated using the DNeasy PowerLyzer PowerSoil Kit (Qiagen). PCR amplification and sequencing were performed at the Australian Genome Research Facility using the primers and conditions outlined in [S1 Table](#). Thermocycling was completed with an Applied Biosystem 384 Veriti and using Platinum SuperFi mastermix (Life Technologies, Australia) for the primary PCR. The first stage PCR was cleaned using magnetic beads, and samples were visualised on 2% Sybr Egel (Thermo-Fisher). A secondary PCR to index the amplicons was performed with TaKaRa PrimeStar Max DNA Polymerase (Clontech). The equimolar pool was cleaned a final time using magnetic beads to concentrate the pool and then measured using a High-Sensitivity D1000 Tape on an Agilent 2200 TapeStation. The pool was diluted to 5nM and molarity was confirmed again using a Qubit High Sensitivity dsDNA assay (ThermoFisher). Amplicons were quantified with a dsDNA fluorometry assay (Promega Quantifluor) after two rounds of PCR. Sequencing took place on an Illumina MiSeq (San Diego, CA, USA) with a V3, 600 cycle kit (2 x 300 base pairs paired-end) and a 25% PhiX spike-in to improve nucleotide diversity. A variation of the Illumina 16S metagenomics sequencing protocol was utilized for this purpose.

2.5 Data analysis

Paired-end reads were assembled by aligning the forward and reverse reads using PEAR (version 0.9.5) [52]. Primers were identified and trimmed before processing using Quantitative Insights into Microbial Ecology (QIIME) [53] USEARCH and UPARSE software [54, 55]. Sequences were quality filtered and full-length duplicate sequences were removed and sorted by abundance using USEARCH with singletons or unique reads in the data set discarded. Sequences were clustered before chimera filtering using the “rdp_gold” database as the reference. To obtain the number of reads in each operational taxonomic unit (OTU), reads were mapped back to OTUs with a minimum identity of 97%. Using QIIME, taxonomy was assigned with the Greengenes database [56].

Community distributions for each site were visualized for the entire samples on phylum, class, order and family level using MEGAN software (MEtaGenome Analyzer) [57]. As sample volumes varied, the number of reads were normalized per 1 ml prior to analysis. Hill numbers were evaluated on family level to gauge the microbial diversity in all samples using Eqs 1–4.

$$H' = - \sum p_i \ln(p_i) \quad (\text{Eq 1})$$

$$\text{Hill}_1 = \exp(H') \quad (\text{Eq 2})$$

$$\gamma = \sum (p_i)^2 \quad (\text{Eq 3})$$

$$\text{Hill}_2 = \frac{1}{\gamma} \quad (\text{Eq 4})$$

Hill₁ uses the exponential of the Shannon-Weaver index H' (Eqs 1 & 2). Hill₂ represents the reciprocal of the Simpson's index γ (Eqs 3 & 4). The number of reads found in the *i*th taxonomic family is depicted by p_i . Visualization of individual bar plots for physicochemical parameters, GHG and nutrient concentrations was carried out using Gnuplot software. Principal component analysis was carried out with Python software in the Spyder IDE with *pandas*, *scikit* and *matplotlib* libraries. To do this, data sets were standardized using StandardScaler() commands and projected into 2 dimensions using PCA() commands (i.e. `pca.fit_transform()`).

After transposition, resulting data sets were individually plotted into the principal subspace of the first 2 principal components (PCs) with *pyplot*.

3 Results

3.1 Physicochemical parameters, nutrients and greenhouse gases

Water temperature showed a maximum of 29.4°C at the estuary mouth (Site 1) and a minimum of 27.4°C at the mixed agriculture site (Site 2). This coincided with an average daytime air temperature of 28.6 ± 1.6 °C on sampling days and only one rainfall event (5.6 mm on the 9th of January, early in the morning). The estuarine salinity gradient decreased from 36.4 at the estuary mouth (Site 1), to 26.6 at the bottom of the weir (Site 5) and dropped to 0.2 at the freshwater site (Site 6) (Fig 2). Water column DO saturation ranged from 90.6% to 106.4% saturation at Sites 1, 4, 5 & 6 (Fig 2), with low DO (26.6–36.8%) observed at the mixed agriculture and urban site (Sites 2 & 3). Pore water DO saturations are assumed to be close to 0% as seen in other study with largely impermeable sediment and high amounts of organic matter [58–60].

DOC concentrations ranged from 0.39 mM at the estuary mouth (Site 1) to 1.8 mM at the freshwater site (Site 6) and had a local maximum of 1.2 mM at the urban site (Site 3) (Fig 3). Ammonium concentrations continuously increased from 22.6 μM at the estuary mouth (Site 1) to 118.7 μM at the freshwater site (Site 6) with the exception of the bottom of the weir (Site 5) where low NH₄⁺ concentrations were observed (4.1 μM). Nitrate concentrations were low at the mixed agriculture, urban sites and sewage treatment plant sites (< 1.5 μM; Sites 2, 3, 4) as well as at the freshwater side of the weir (Site 6) with only the bottom of the weir (Site 5) showing relatively high nitrate concentrations (46.5 μM). Sulfate concentrations in pore water were lowest at the freshwater site (0.03 mM; Site 6) and ranged from 1.7 to 3.3 mM at the other sites but did not follow the salinity gradient. Nutrient data from surface water samples revealed no relationship to relevant porewater communities (refer to S2 Fig).

CH₄ concentrations in the estuary varied widely along the salinity and land use gradient with concentrations ranging from 0.2 ± 0.01 μM at the estuary mouth (Site 1) to 2.68 ± 0.2 μM at the freshwater site (Site 6) (Fig 4). Downstream of the weir, maximum CH₄ concentrations were observed in the water column at the urban site (Site 3; 0.51 ± 0.04 μM) and the sewage treatment plant (Site 4; 0.66 ± 0.11 μM). CO₂ concentrations in the water column were highest at the urban site (Site 3; 212 ± 14 μM) and ranged from 14 μM to 54 μM at all other sites (Fig 4). Both CH₄ and CO₂ concentrations were only measured in the water column at a fixed depth (0.5–0.7 m) due to the sampling design. Additional oxidation of gas fluxes prior to reaching the water column sampling location thus need to be considered for pore water processes.

3.2 Prokaryotic community composition and diversity

There were notable differences in community distribution on phylum level between the surface and pore water samples within each site, as well as trends along the estuarine land use gradient (Fig 5). *Cyanobacterial* OTUs mainly occurred in surface water samples and were most prevalent at the mouth of the estuary with decreasing relative abundance along the salinity gradient up to the weir and were low at the mixed agriculture site and urban site (Sites 2 & 3) where DO was low. The functionally diverse *Proteobacteria* were abundant in all samples. Differences in community distributions were especially pronounced in the pore water samples with an increased relative abundance of *Firmicutes*, *Euryarchaeota* and *Chloroflexi* in the urban sites (Sites 3 & 4). The *Euryarchaeota* phylum includes a variety of methanogens with six of the seven known orders of methanogenic archaea detected in this study

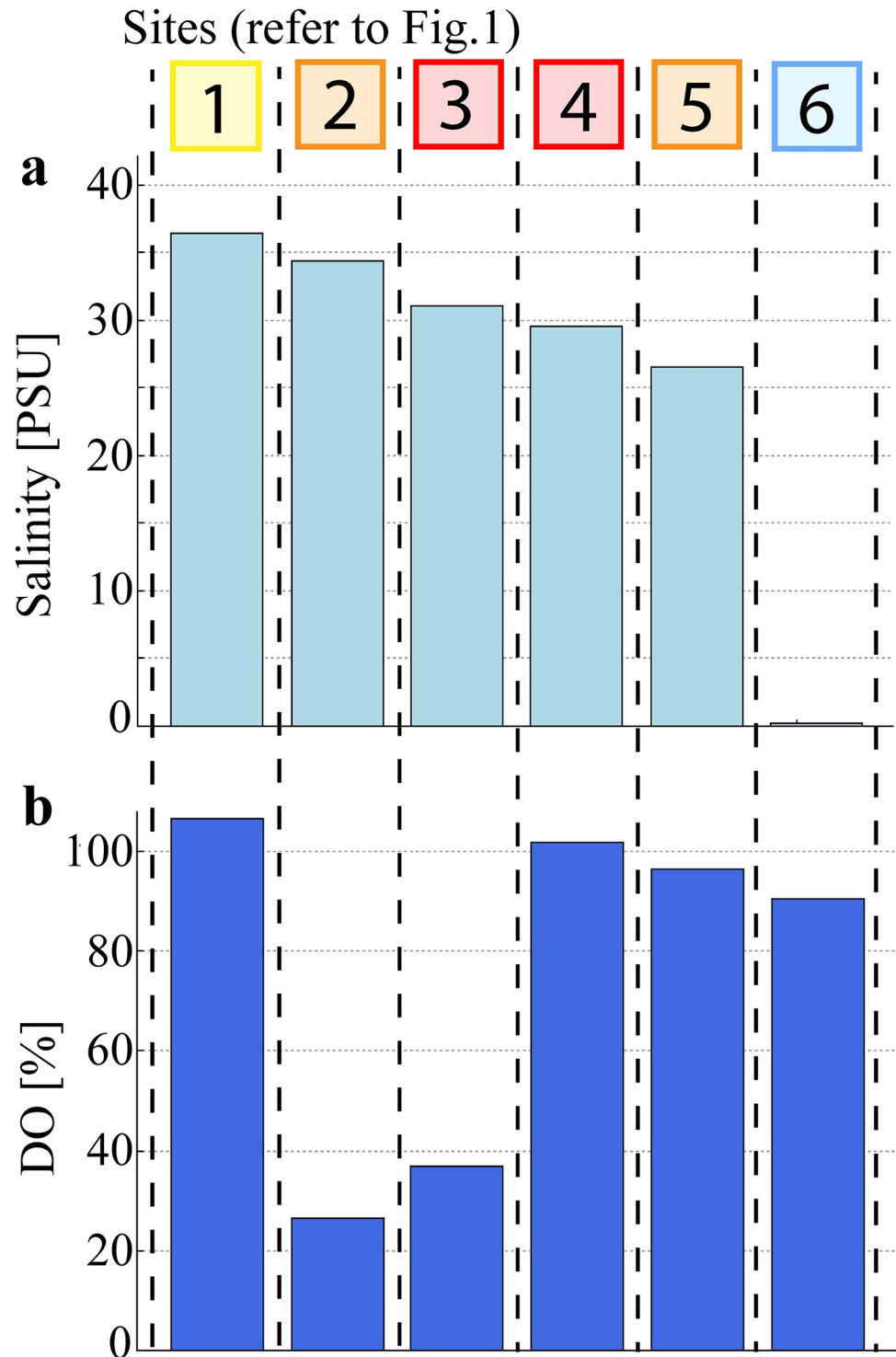


Fig 2. Average physicochemical parameters in the water column of the Burnett River estuary for each site.

<https://doi.org/10.1371/journal.pone.0242339.g002>

(*Methanobacteriales*, *Methanocellales*, *Methanococcales*, *Methanomassiliicoccales*, *Methanomicrobiales* and *Methanosarcinales*) [19, 61] (refer to Fig 6). The Chloroflexi phylum was dominated by the dehalogenating order *Dehalococcoidales* which have been previously depicted as

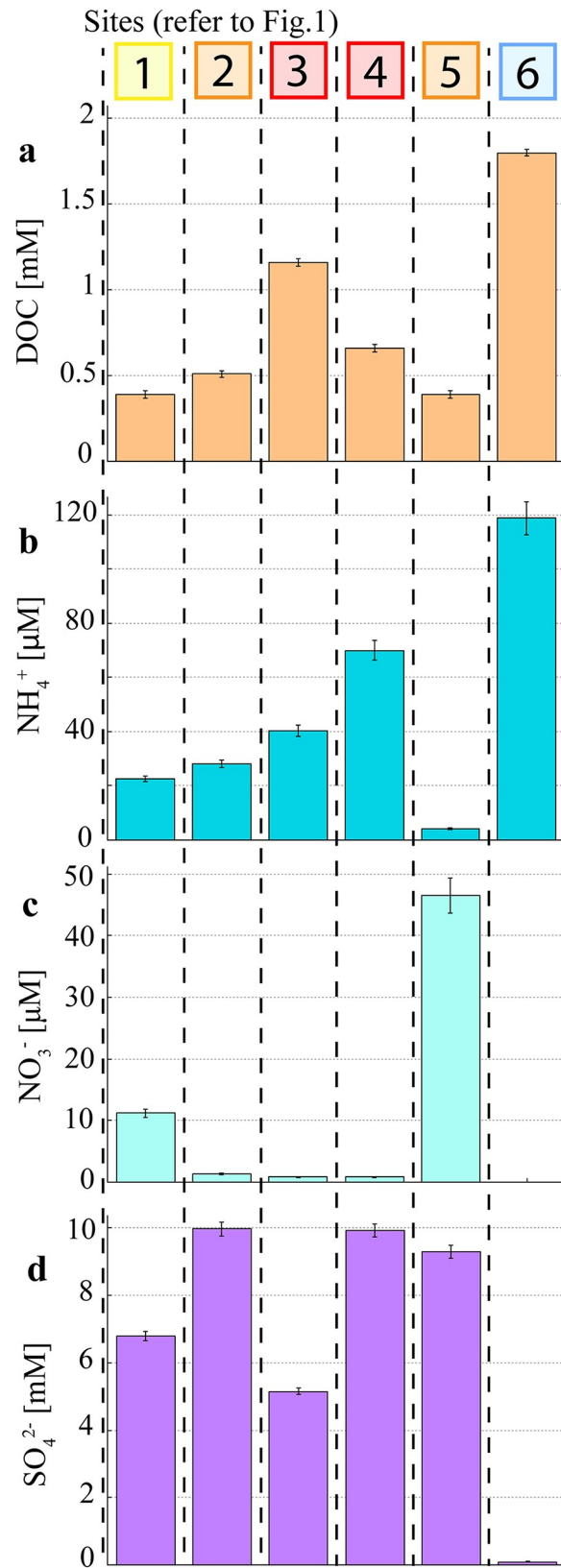


Fig 3. Pore water nutrient concentrations at the different sites along the Burnett River estuary.

<https://doi.org/10.1371/journal.pone.0242339.g003>

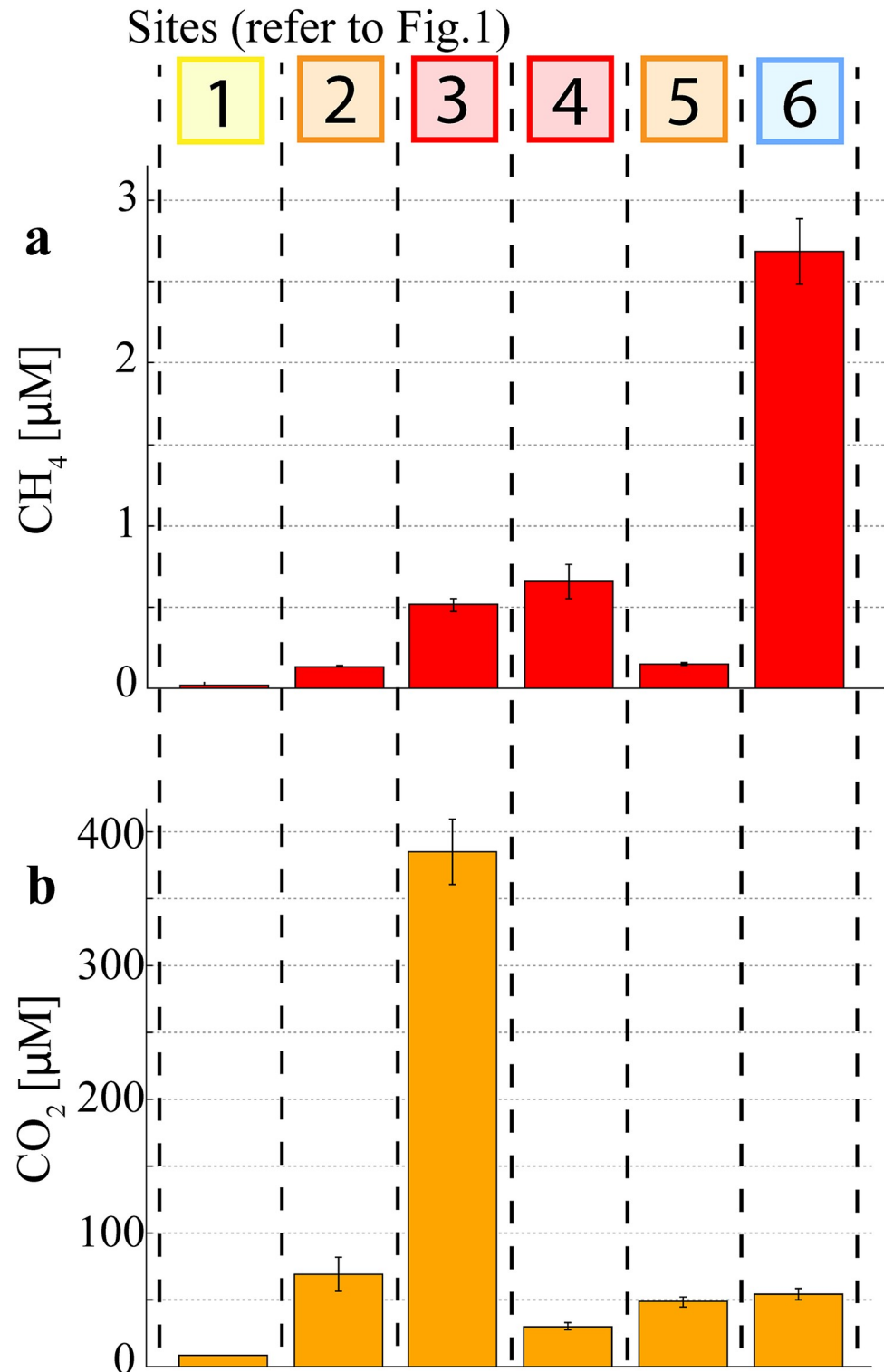


Fig 4. Water column greenhouse gas concentrations along the Burnett estuary land use gradient. Note: Error bars represent \pm SD of averaged data from CRDS.

<https://doi.org/10.1371/journal.pone.0242339.g004>

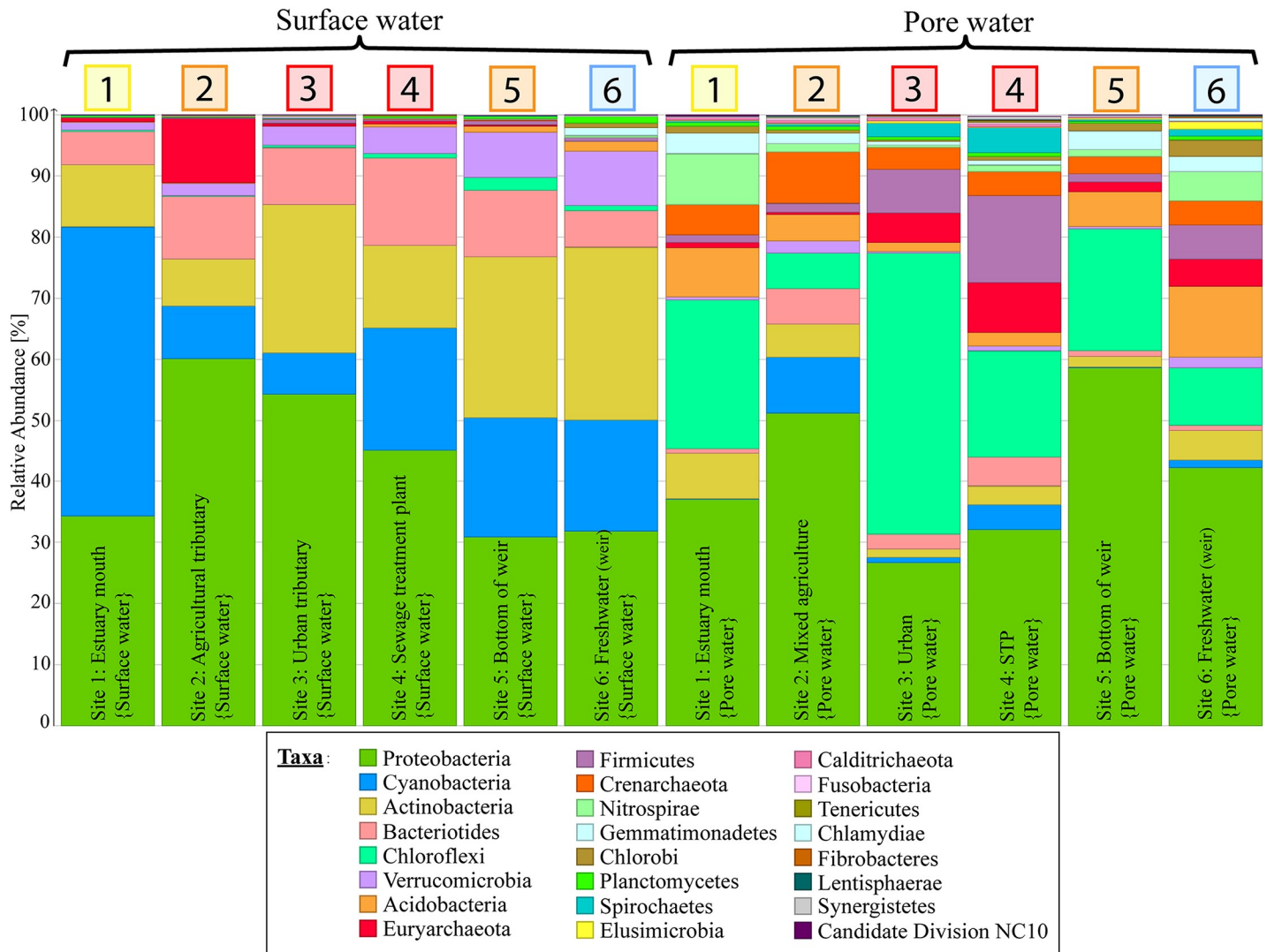


Fig 5. Community bar plot of prevalent prokaryotic phyla in the Burnett River estuary. Relative abundances are depicted for each phylum per sampling site. Phyla with an abundance of <0.1% in all individual samples were discarded.

<https://doi.org/10.1371/journal.pone.0242339.g005>

bioremediation bacteria in polluted environments [62–64]. Notably, the total number of dsDNA detected per ml varied between samples and ranged from 5,027 at the urban site (Site 3) to 12,346 at the freshwater site (Site 6) in surface water samples and between 6,967 at the bottom of the weir (Site 5) and 14,743 at the mixed agriculture site (Site 2) in pore water samples (S2 Table).

In surface water samples, the diversity indexed by Hill₁ (more weight on OTU richness) and Hill₂ (more weight on OTU evenness) was highest at the urban site (Site 3; Hill₁ = 75.2, Hill₂ = 12.2) and lowest at the estuary mouth (Site 1) (Hill₁ = 4.9, Hill₂ = 1.7) (Table 1). Average diversity in pore water samples was overall higher (Hill_{1,AVG} = 72.6 ± 42.2, Hill_{2,AVG} = 10.2 ± 5.6) than surface water samples (Hill_{1,AVG} = 39.9 ± 22.3, Hill_{2,AVG} = 6.7 ± 2.5) with the highest values at the sewage treatment plant (Site 4; Hill₁ = 123.4, Hill₂ = 17.7) and the lowest diversity observed at the bottom of the weir (Site 5; Hill₁ = 22.3, Hill₂ = 3.6) (Table 1). Diversity trends followed the land use gradient with more diverse communities occurring in the

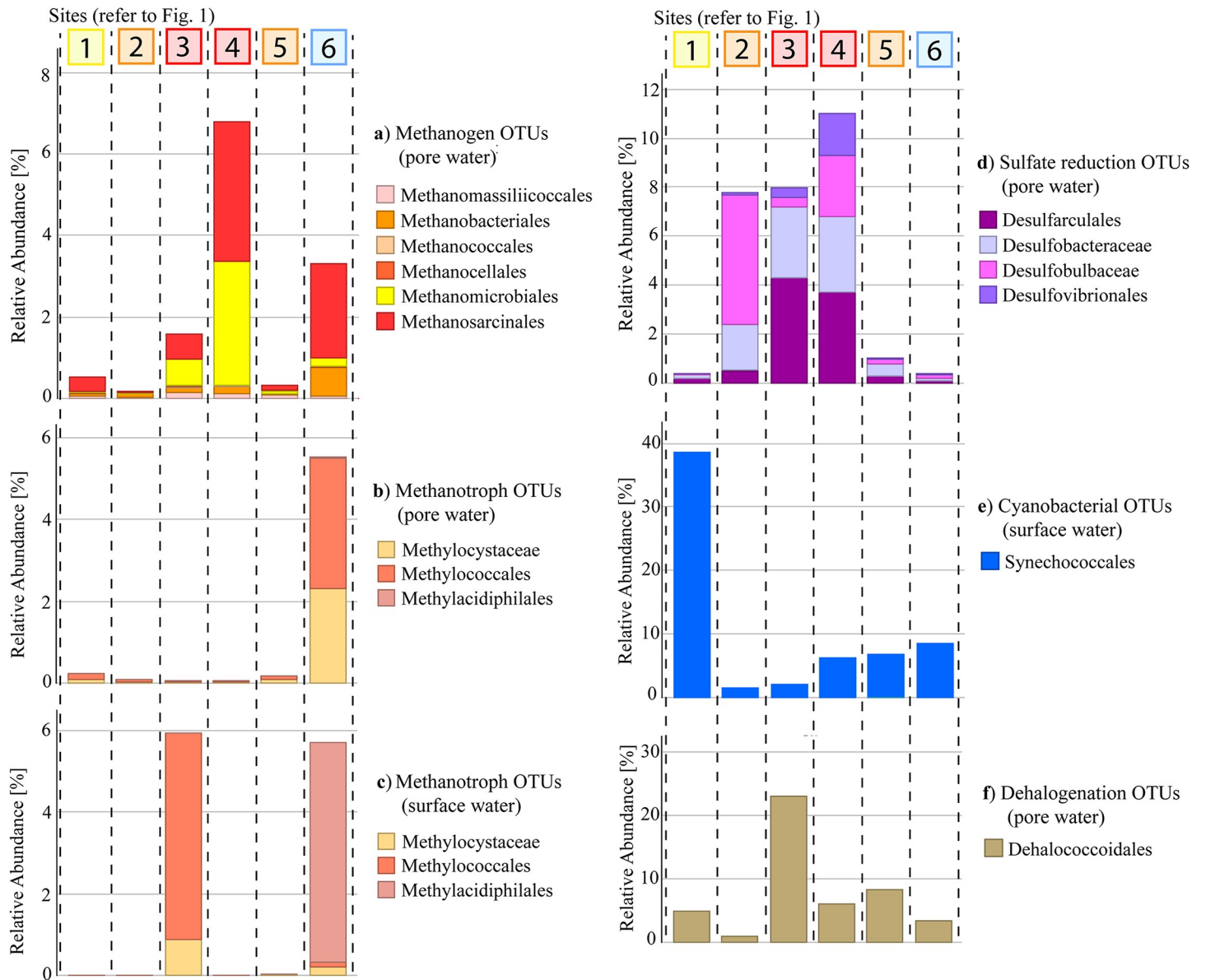


Fig 6. The relative abundances of select environmental OTUs along a land use gradient in the Burnett River estuary. Functional groups were combined in the stacked bar plots.

<https://doi.org/10.1371/journal.pone.0242339.g006>

agricultural and urban sites (Sites 2 & 3) around the city centre as well as at the freshwater side of the weir (Site 6). Exceptions to this trend were found in the diversity of prokaryotic communities in STP (Site 4) surface water samples and urban (Site 3) pore water samples.

Table 1. Hill numbers of diversity indices calculated for all sites in surface and pore water. Hill₀ represents the detected number of OTUs for each sample.

Site	Surface water samples						Pore water samples					
	1	2	3	4	5	6	1	2	3	4	5	6
Hill ₀	92	111	151	107	128	129	125	135	119	135	121	136
Hill ₁	4.9	19.1	75.2	28.7	41.7	69.6	42.9	117.92	26.1	123.4	22.3	103.0
Hill ₂	1.7	4.3	12.2	6.7	8.3	7.0	6.26	15.3	3.7	17.7	3.6	14.2

<https://doi.org/10.1371/journal.pone.0242339.t001>

3.3 Environmental OTUs

Prokaryotic pore water communities shifted towards methanogenic archaea along the land use gradient (Fig 6). Methanogenic archaea in anoxic pore water samples showed a higher relative abundance at the urban site (Site 3) and sewage treatment plant site (Site 4) as well as the freshwater site (Site 6). Relative abundances of pore water methanogenic archaea ranged from 0.2% at the mixed agriculture site (Site 2) to 7.8% near the sewage treatment plant (Site 4). The relative abundance of methanogenic archaea in pore water samples from the freshwater site (Site 6), which corresponded to the highest CH₄ and DOC concentrations (Figs 3A & 4A), was only 3.3%, but the total number of reads from freshwater site (Site 6) pore water samples was 38% higher than at the urban site (Site 3) (see S2 Table). Methanogenic archaea detected in surface water were below 0.01% (or 25 reads) and thus not further considered. The proportion of methanotroph OTUs was highest at the freshwater site (Site 6) in surface and pore water samples (relative abundances of 5.7% and 5.6% respectively) and in urban (Site 3) surface water samples (relative abundance of 5.9%; lowest total number of reads). Freshwater (Site 6) surface water samples were the only ones dominated by the thermoacidophilic methanotroph order *Methylacidiphilales*, with only a low fraction of type I or type II methanotrophs. The relative abundance of methanotrophs was below 0.5% at all other sites. All detected methanotrophic prokaryotes belonged to the bacteria kingdom with no ANME (anaerobic methanotrophic archaea) found in any of the samples. Denitrifying anaerobic methane oxidation (DAMO) bacteria belonging to the *Candidate Division NC10* phylum were detected in Site 1 pore water samples but had a low relative abundance of ~0.3%.

Coinciding with relatively high concentrations of DOC (> 0.5 mM) in pore water at Sites 2, 3 and 4, the relative abundance of sulfate reducing OTUs ranged from 7.8% to 10.5% and was below 1% at all other sites. The relative abundance of the dehalogenation OTU *Dehalococcoidales* (accounting for 99.9% of *Chloroflexi*) was highest at the urban dominated Site 3 (22.9%) and ranged from 1.0% to 8.1% at all other sites. *Synechococcales* was the most abundantly occurring order of the *Cyanobacteria* phylum (accounting for 99.8% of *Cyanobacteria*) in surface water samples and had the highest relative abundance (39.1%) at the mouth of the estuary (Site 1) and the lowest at the mixed agriculture and urban sites (Sites 2 & 3; 1.5% and 2% relative abundance respectively) where DO saturation was the lowest.

4 Discussion

Prokaryotic communities showed distinct changes in taxonomic profiles between land use types as well as along the estuarine salinity gradient within the Burnett River estuary. In particular, we found the highest abundance of methanogenic archaea in the urban and STP sites (Sites 3 and 4) of the estuary (Fig 6), which corresponded to elevated CH₄ and CO₂ concentrations (Fig 4). In other urbanised catchments, the presence of elevated concentrations of DOC coupled with an absence of thermodynamically favourable electron acceptors has been shown to facilitate the proliferation of methanogenic archaea [14, 65, 66]. This implies that increased inputs of organic matter due to catchment urbanisation and modification may lead to an increase in methanogenesis and GHG production [11, 12].

Principal component analysis (Fig 7) supports the strong relationship between pore water methanogens and DOC concentrations, as well as water column CO₂ concentrations, which can be used as energy sources for CH₄ generation [14, 28]. The abundance of methanogens however did not gradually increase moving upstream along the salinity gradient as observed in previous studies [41, 67, 68]. Conversely, urban and sewage related high DOC concentrations and scarcity of thermodynamically favourable electron acceptors (e.g. DO, NO₃⁻) in the pore water appear to cause a stark shift in prokaryotic community compositions, with the highest

abundance of methanogens found adjacent to the STP (Site 4; refer to Fig 6). Highly labile DOC compounds from sewage related run-off are subject to rapid microbial degradation and have been previously shown to increase methane abundance [69]. This suggests that land use differences along the estuary may have a stronger effect on prokaryotic community structure than the salinity gradient alone. Conversely, aerobic conditions in the surface water (DO concentrations of 26.6% to 106.4%; Fig 2) limit methanogen communities to the anoxic pore water.

In the archaeal communities, the relative abundances of detected methanogenic orders belonging to the *Euryarchaeota* phylum varied between sites. For example, there was a 5 to 15 times lower relative abundance of *Methanomicrobiales* and a 4 to 8 times higher relative abundance of *Methanobacteriales* in the freshwater site (Site 6) compared to the urban and STP sites (Sites 3 & 4). The metabolically diverse *Methanosarcinales* had a high relative abundance in pore water samples at all sites where methane concentrations were high (between 41% and 68% of total methanogen communities at Sites 3, 4 and 6). Differences in the relative abundances of these *Euryarchaeota* may have contributed to changes in CH₄ concentrations at the sites with a high relative abundance of methanogens. The PCA plot reveals that *Methanobacteriales* and *Methanocellales* follow the DOC gradient, whereas *Methanococcales*, *Methanomasiliicoccales*, *Methanomicrobiales* and *Methanosarcinales* more closely follow the CO₂ gradient (Fig 7). The methanogen OTUs that follow the CO₂ gradient show clustering with sulfate reducing OTUs as well as the with the urban and STP sites (Site 3 & 4) and could thus be the main drivers of the observed local maxima in GHG production at these sites.

There was a considerably higher abundance of the order *Methanobacteriales* in the freshwater (Site 6) samples, where the highest CH₄ concentrations were seen (2.68 μM). Conversely, the *Methanomicrobiales* order had the highest abundance at the sewage treatment plant (Site 4), where the highest CH₄ concentrations along the estuarine salinity gradient were observed (0.66 μM; Sites 1–5) (Fig 4). As there is almost no sulfate (Fig 3) and a low relative abundance of sulfate reducers (Fig 6) present at the freshwater site (Site 6), a lack of competition for hydrogen produced by fermenters in the anoxic pore water could explain higher methane production rates of methanogens which commonly use H₂ as an electron donor [34, 70]. Further, differences in methane production rates between orders could contribute to the observed differences between CH₄ concentrations at the freshwater site (Site 6) and the other sites (Sites 1–5). The quantification of methane production rates of different methanogenesis taxa is still lacking in the literature owing to difficulties in culturing most of these microorganisms [6, 19, 71]. To narrow down contributions of individual methanogenic OTUs, amplicon sequencing data and in situ CH₄ concentrations could be combined with further microbiological methodology like shotgun metagenomics or transcriptomics to gauge the abundance and/or expression of methanogenesis genes (e.g. the *mcrA* gene) in the environment.

Within the more impacted urban and STP sites (Sites 3 and 4), there was a co-occurrence of high relative abundances of sulfate reducing bacteria and methanogenic archaea in pore water, pointing to a potential syntrophic relationship between the two groups. Sulfate reducing bacteria have a high affinity to hydrogen and acetate and readily outcompete methanogens for these common electron donors [40, 70]. A high loading of labile DOC compounds in the substrate however can limit competition and allow for co-existence of sulfate reducing bacteria and methanogenic archaea [34, 40, 72]. The high concentration of DOC in the urban environment around Bundaberg (i.e. urban/STP, Sites 3 & 4) thus seems to prevent sulfate reducers and methanogens from outcompeting each other and enable substantial communities of both functional groups to co-exist and form syntrophic relationships. These results also point to a low concentration of humic substances in the DOC, which have been shown to inhibit both

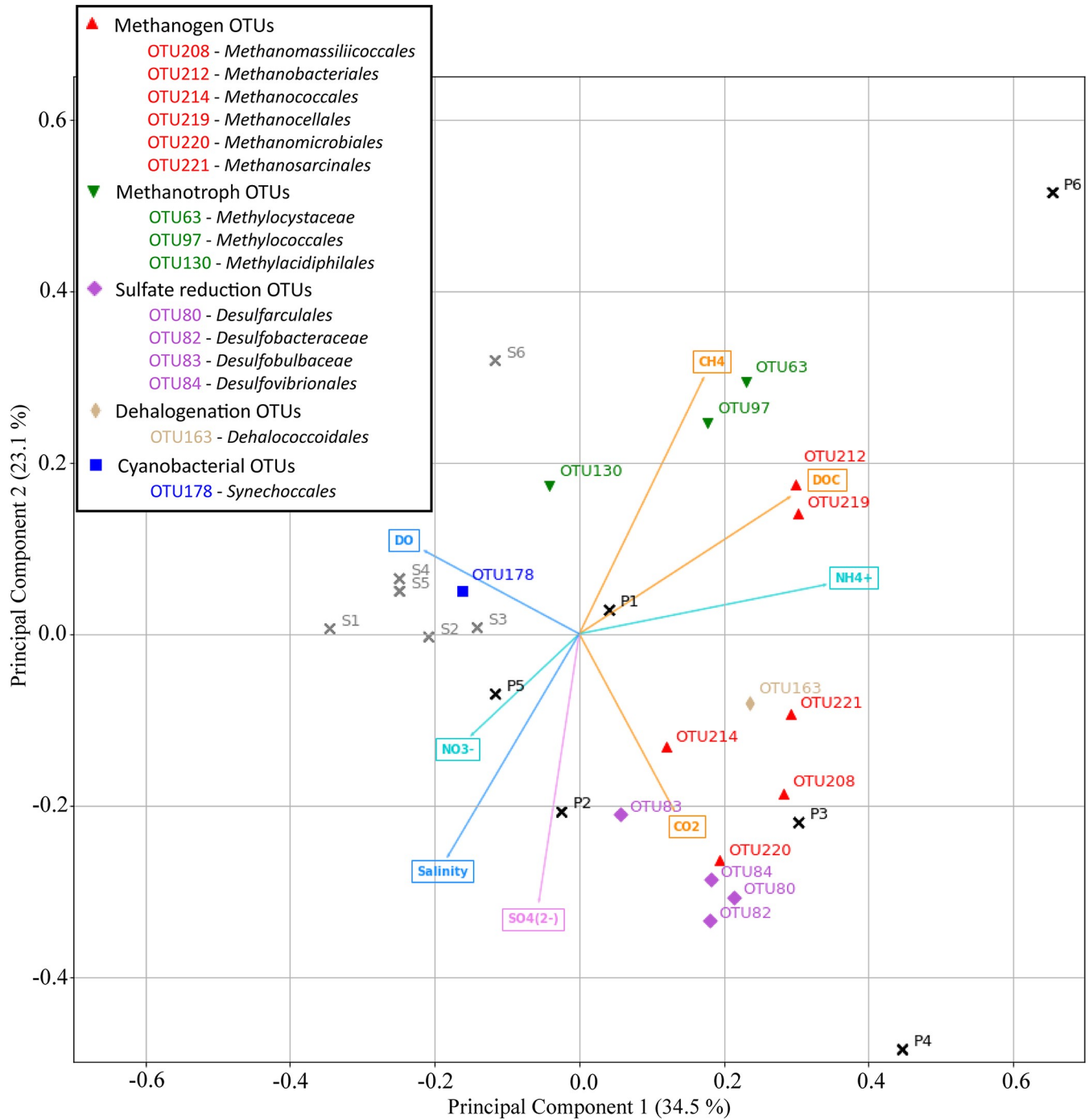


Fig 7. PCA biplot depicting variations in environmental parameters (nutrient, greenhouse gas and physicochemical). OTUs included in the scatter plot are specified on the upper left. Surface water samples for Sites 1–6 are shown as grey crosses with the suffix 'S' and pore water samples are depicted as black crosses with the suffix 'P'.

<https://doi.org/10.1371/journal.pone.0242339.g007>

methanogenesis and sulfate reduction as well as serve as an electron acceptor for ANME (absent in our samples; see section 3.3) [73–75].

The study also found high CO₂ concentrations in the most impacted sites (i.e. urban/STP, Sites 3 & 4) which can fuel microbially mediated methane generation. Sulfate reducers can

account for almost 100% of total CO₂ (via production of bicarbonate) in polluted mangrove sediments [5, 76]. This CO₂ can fuel methanogenesis if methanogens find a favourable substrate to proliferate [14, 32, 77]. That is reflected by a high abundance of both sulfate reducing bacteria (7.8% to 10.5%) and methanogenic archaea (7.8% at Site 4) as well as high concentrations of CH₄ (0.51 to 0.66 μM) and CO₂ (212 μM at Site 3) in the urban and STP sites (Sites 3 & 4) of the estuary. Urbanized estuaries could thus facilitate a GHG-fuelled microbial loop between methanogenic archaea and sulfate reducing bacteria that drastically increases CH₄ and CO₂ emissions in these environments. However, the exact mechanism of interplay between individual OTUs which is resulting in increased GHG concentrations along estuarine land use gradients was not determined.

A lack of NO₃⁻ was detected in the more impacted sites where high relative abundances of methanogens and sulfate reducers were observed in pore water (urban/STP, Sites 3 & 4). Conversely, NO₃⁻ concentrations were high (46.5 μM) in the pore water at the bottom of the weir (Site 5; inland macadamia agriculture) where low concentrations of CH₄ (< 0.15 μM) and CO₂ (< 0.03 μM) were detected. PCA analysis shows the inverse relationship between NO₃⁻ and CH₄ dynamics, highlighting the inhibition of methanogenesis at the bottom of the weir (Site 5) (Fig 7). Relatively low NH₄⁺ concentrations (4.1 μM) were also observed in the high NO₃⁻ containing pore water samples downstream of the weir (Site 5). Anaerobic ammonium oxidation (anammox) can build up NO₂⁻, an intermediate in the production of NO₃⁻ that is toxic to methanogens [38, 78]. In previous studies, high NO₃⁻ concentrations have also been linked to the inhibition of CH₄ generation due to denitrification bacteria outcompeting methanogens [35, 38, 79]. Fang et al. [79] showed in an upflow anaerobic sludge blanket reactor which was treating wastewater containing phenol, that methanogenesis only occurred after all denitrification had been carried out in the substrate and only if organic material (measured via chemical oxygen demand to NO₃⁻-N ratios) was still available after fuelling the denitrification bacteria.

We found a concomitant relationship between the high abundance of methanotrophs and CH₄ at the urban and freshwater sites (Site 3 and 6). Pore water methanotrophs have distinct differences in phylogeny, with the recently discovered *Methylacidiphilales* order representing a majority of taxa at the freshwater site (Site 6) while being largely absent at all other sites. The potential existence of distinct microenvironments entailing different pH could explain the prevalence of acidophilic *Methylacidiphilales* at the freshwater site [80, 81]. Varying rates of CH₄ oxidation in different taxa could be hypothesized to contribute to observed differences in CH₄ concentrations. However, methanotrophic microorganisms have not yet been well characterized [82]. Additional research focussing on environmental methanotrophs could include the isolation of environmental samples containing a high proportion of a single methanotroph OTU (e.g. *Methylacidiphilales*). The abundance of these methanotrophs could subsequently be determined together with CH₄ oxidation rates in the samples which could allow for a quantitative link between rates and OTUs. It is also noted, that total abundance measurements via PCR-based methods are generally error-prone and further research could be improved by employing additional quantification assays like flow cytometry [83–86].

At the mouth of the estuary, the relative abundance of cyanobacterial OTU (*Synechococcales*) was 4 to 20 times higher than in the other surface water samples (38%; Site 1). This is likely due to oceanic *Synechococcus* sp. dominated communities transported into the estuary during each tide as has been reported previously [87]. Relative abundances of photosynthetic bacterioplankton in surface water communities of the estuary were closely associated with physicochemical gradients [21, 88]. The dehalogenation OTU *Dehalococcoidales* had a strong inverse relationship to *Cyanobacteria* and the physicochemical gradients in the PCA plot (Fig 7). This occurred prominently at the urban site (Site 3) and almost exclusively in pore water

samples, suggesting its potential use as a marker taxon for urban and industrial run off. *Dehalococcoidales* may also play an important role in the bioremediation of harmful compounds (e.g. Chlorobenzenes and chloroethylenes) discharging into the potentially sensitive GBR marine park [62, 64]. Torlapati et al. [64] revealed an acceleration of dechlorination and bioremediation when bacterial growth of *Dehalococcoides sp.* was increased in an artificial groundwater aquifer.

The main driver of GHG cycling prokaryote distributions was likely the carbon biogeochemistry along the land use gradient, and especially in the urban, STP and freshwater environments (Sites 3, 4 & 6). Most of the investigated OTUs and urban pore water samples are aligned with the carbon compounds (Fig 7). This is also apparent in individual bar plots of prokaryotes (Fig 6A, 6D and 6F) and carbon compounds (Figs 3A, 4A and 4B) which all have local maxima at the sites with a higher urbanisation (urban/STP, Sites 3 & 4). Diversity indices of the entire microbial communities also showed increased values at highly impacted sites rather than following physicochemical gradients (Table 1). This implies a lowered significance of the physicochemical parameters which are commonly depicted as the main driving forces of microbial community compositions in estuarine environments [21, 22].

Overall, this study highlights the relationship between the distribution of microbial communities and GHG dynamics along an estuarine land use gradient. Most microbes are restricted to specific niches in the environment they live in [32, 89, 90]. Physicochemical parameters like DO and salinity impact these niches as described in previous studies [21, 23] and correspondingly evoked changes in microbial communities along the Burnett River estuary. However, the shift in community compositions along the Burnett River estuary seemed to be highly influenced by urban land use zones which had a general scarcity of nutrients but elevated concentrations of carbon compounds. The changes in land use resulted in distinct ecological niches that likely facilitated the proliferation of methanogenic archaea and sulfate reducers as well as leading to considerable increases in GHG concentrations. More research on how land use mediates shifts in environmental parameters and microbial communities within these ecological niches needs to be carried out to better understand GHG emission and nutrient fluxes to sensitive ecosystems such as the GBR. Additionally, specific OTUs and genes involved in GHG dynamics in these vulnerable coastal ecosystems need to be characterized further.

Supporting information

S1 Table. Thermal cycling lengths with temperatures and primers used for the PCR procedure.

(DOCX)

S2 Table. Total number of dsDNA per ml of each sample, quantified by fluorometry (see section 2.3).

(DOCX)

S1 Fig. Hierarchical clustering plot using negative Pearson correlation metrics for a) pore water samples (sampling sites numbered P1 –P6) and b) surface water samples (sampling sites numbered S1 –S6); Duplicates are denoted after sample numbers in blue. Dissimilarity heights (≥ 0.01) between duplicates are shown in green.

(TIF)

S2 Fig. Surface water nutrient concentrations at the different sites along the Burnett River estuary. No direct links to relevant prokaryotic pore water communities.

(TIF)

S1 Data.

(CSV)

S2 Data.

(CSV)

S3 Data.

(CSV)

Author Contributions**Conceptualization:** Sebastian Euler, Luke C. Jeffrey, Douglas R. Tait.**Data curation:** Sebastian Euler, Damien T. Maher, Douglas R. Tait.**Formal analysis:** Sebastian Euler.**Funding acquisition:** Sebastian Euler, Douglas R. Tait.**Investigation:** Sebastian Euler, Luke C. Jeffrey, Derek Mackenzie.**Methodology:** Sebastian Euler, Luke C. Jeffrey, Damien T. Maher, Douglas R. Tait.**Project administration:** Sebastian Euler, Douglas R. Tait.**Resources:** Sebastian Euler, Luke C. Jeffrey, Damien T. Maher, Derek Mackenzie.**Software:** Sebastian Euler, Luke C. Jeffrey.**Supervision:** Damien T. Maher, Douglas R. Tait.**Validation:** Sebastian Euler, Damien T. Maher, Douglas R. Tait.**Visualization:** Sebastian Euler.**Writing – original draft:** Sebastian Euler.**Writing – review & editing:** Luke C. Jeffrey, Damien T. Maher, Douglas R. Tait.**References**

1. Canuel EA, Cammer SS, McIntosh HA, Pondell CR. Climate Change Impacts on the Organic Carbon Cycle at the Land-Ocean Interface. *Annu Rev Earth Planet Sci.* 2012; 40(1):685–711. <https://doi.org/10.1146/annurev-earth-042711-105511>
2. Abril G, Borges AV. Carbon Dioxide and Methane Emissions from Estuaries. In: Tremblay A, Varfalvy L, Roehm C, Garneau M, editors. *Greenhouse Gas Emissions—Fluxes and Processes: Hydroelectric Reservoirs and Natural Environments.* Berlin, Heidelberg: Springer Berlin Heidelberg; 2005. p. 187–207.
3. Bianchi TS. *Biogeochemistry of Estuaries.* Oxford University Press, USA; 2007. 706 p.
4. Brankovits D, Pohlman JW, Niemann H, Leigh MB, Leewis MC, Becker KW, et al. Methane- and dissolved organic carbon-fueled microbial loop supports a tropical subterranean estuary ecosystem. *Nat Commun.* 2017; 8(1):1835. <https://doi.org/10.1038/s41467-017-01776-x> PMID: 29180666
5. Li Y, Zheng L, Zhang Y, Liu H, Jing H. Comparative metagenomics study reveals pollution induced changes of microbial genes in mangrove sediments. *Sci Rep.* 2019; 9(1):5739. <https://doi.org/10.1038/s41598-019-42260-4> PMID: 30952929
6. Baker BJ, Lazar CS, Teske AP, Dick GJ. Genomic resolution of linkages in carbon, nitrogen, and sulfur cycling among widespread estuary sediment bacteria. *Microbiome.* 2015; 3:14. <https://doi.org/10.1186/s40168-015-0077-6> PMID: 25922666
7. Looman A, Santos IR, Tait DR, Webb J, Holloway C, Maher DT. Dissolved carbon, greenhouse gases, and $\delta^{13}\text{C}$ dynamics in four estuaries across a land use gradient. *Aquat Sci.* 2019; 81(1):22. <https://doi.org/10.1007/s00027-018-0617-9>

8. Chuang PC, Young MB, Dale AW, Miller LG, Herrera-Silveira JA, Paytan A. Methane fluxes from tropical coastal lagoons surrounded by mangroves, Yucatán, Mexico: Methane Fluxes from Coastal Lagoons. *J Geophys Res Biogeosci*. 2017; 122(5):1156–74. <https://doi.org/10.1002/2017JG003761>
9. Pachauri RK, Allen MR, Barros VR, Broome J, Cramer W, Christ R, et al. Climate Change 2014: Synthesis Report. Contribution of Working Groups I, II and III to the Fifth Assessment Report of the Intergovernmental Panel on Climate Change. Geneva, Switzerland: IPCC; 2014. 2014.
10. Borges AV. Do we have enough pieces of the jigsaw to integrate CO₂ fluxes in the coastal ocean? *Estuaries*. 2005; 28(1):3–27. <https://doi.org/10.1007/BF02732750>
11. Reading MJ, Tait DR, Maher DT, Jeffrey LC, Looman A, Holloway C, et al. Land use drives nitrous oxide dynamics in estuaries on regional and global scales. *Limnol Oceanogr*. 2020;n/a(n/a). <https://doi.org/10.1002/lno.11426>
12. Brigham BA, Bird JA, Juhl AR, Zappa CJ, Montero AD, O'Mullan GD. Anthropogenic inputs from a coastal megacity are linked to greenhouse gas concentrations in the surrounding estuary. *Limnol Oceanogr*. 2019; 64(6):2497–511. <https://doi.org/10.1002/lno.11200>
13. Ramachandran R, Ganapathiagraharam Ramachandran P, Danesh Chand P, Prabhat Kumar G, Ashesh Prasad M. Anthropogenic Forcing on Methane Efflux from Polluted Wetlands (Adyar River) of Madras City, India. *Ambio*. 1997; 26(6):369–74.
14. Lyu Z, Shao N, Akinyemi T, Whitman WB. Methanogenesis. *Curr Biol*. 2018; 28(13):R727–R32. <https://doi.org/10.1016/j.cub.2018.05.021> PMID: 29990451
15. Kirschke S, Bousquet P, Ciais P, Saunois M, Canadell JG, Dlugokencky EJ, et al. Three decades of global methane sources and sinks. *Nat Geosci*. 2013; 6(10):813–23. <https://doi.org/10.1038/ngeo1955>
16. Nisbet EG, Manning MR, others. Very strong atmospheric methane growth in the 4 years 2014–2017: Implications for the Paris Agreement. *Global*. 2019.
17. Maher DT, Eyre BD. Carbon budgets for three autotrophic Australian estuaries: implications for global estimates of the coastal air-water CO₂ flux. *Global Biogeochemical Cycles: An International Journal of Global Change*. 2012; 26(1). <https://doi.org/10.1029/2011GB004075>
18. Pace NR. A molecular view of microbial diversity and the biosphere. *Science*. 1997; 276(5313):734–40. <https://doi.org/10.1126/science.276.5313.734> PMID: 9115194
19. Liu Y, Whitman WB. Metabolic, phylogenetic, and ecological diversity of the methanogenic archaea. *Ann N Y Acad Sci*. 2008; 1125:171–89. <https://doi.org/10.1196/annals.1419.019> PMID: 18378594
20. Telesh IV, Khlebovich VV. Principal processes within the estuarine salinity gradient: a review. *Mar Pollut Bull*. 2010; 61(4–6):149–55. <https://doi.org/10.1016/j.marpolbul.2010.02.008> PMID: 20304437
21. Liu J, Fu B, Yang H, Zhao M, He B, Zhang X-H. Phylogenetic shifts of bacterioplankton community composition along the Pearl Estuary: the potential impact of hypoxia and nutrients. *Front Microbiol*. 2015; 6:64. <https://doi.org/10.3389/fmicb.2015.00064> PMID: 25713564
22. Hong Y, Wu J, Wilson S, Song B. Vertical Stratification of Sediment Microbial Communities Along Geochemical Gradients of a Subterranean Estuary Located at the Gloucester Beach of Virginia, United States. *Front Microbiol*. 2018; 9:3343. <https://doi.org/10.3389/fmicb.2018.03343> PMID: 30687299
23. Yang J, Ma La, Jiang H, Wu G, Dong H. Salinity shapes microbial diversity and community structure in surface sediments of the Qinghai-Tibetan Lakes. *Sci Rep*. 2016; 6:25078. <https://doi.org/10.1038/srep25078> PMID: 27113678
24. Abatenh E, Gizaw B, Tsegaye Z, Tefera G. Microbial Function on Climate Change—A Review. *Environment Pollution and Climate Change*. 2018; 2(1):1–6. <https://doi.org/10.4172/2573-458X.1000147>
25. Murrell JC, Jetten MSM. The microbial methane cycle. *Environ Microbiol Rep*. 2009; 1(5):279–84. <https://doi.org/10.1111/j.1758-2229.2009.00089.x> PMID: 23765880
26. Pires ACC, Cleary DFR, Almeida A, Cunha A, Dealtry S, Mendonça-Hagler LCS, et al. Denaturing gradient gel electrophoresis and barcoded pyrosequencing reveal unprecedented archaeal diversity in mangrove sediment and rhizosphere samples. *Appl Environ Microbiol*. 2012; 78(16):5520–8. <https://doi.org/10.1128/AEM.00386-12> PMID: 22660713
27. Taketani RG, Yoshiura CA, Dias ACF, Andreote FD, Tsai SM. Diversity and identification of methanogenic archaea and sulphate-reducing bacteria in sediments from a pristine tropical mangrove. *Antonie Van Leeuwenhoek*. 2010; 97(4):401–11. <https://doi.org/10.1007/s10482-010-9422-8> PMID: 20195901
28. Torres-Alvarado MdR Fernández FJ, Ramírez Vives F, Varona-Cordero F. Dynamics of the methanogenic archaea in tropical estuarine sediments. *Archaea*. 2013; 2013:582646. <https://doi.org/10.1155/2013/582646> PMID: 23401664
29. Deppenmeier U, Müller V. Life close to the thermodynamic limit: how methanogenic archaea conserve energy. *Results Probl Cell Differ*. 2008; 45:123–52. https://doi.org/10.1007/400_2006_026 PMID: 17713742

30. Mohd Yasin NH, Maeda T, Hu A, Yu C-P, Wood TK. CO₂ sequestration by methanogens in activated sludge for methane production. *Appl Energy*. 2015; 142:426–34. <https://doi.org/10.1016/j.apenergy.2014.12.069>
31. Wang J, Liu H, Fu B, Xu K, Chen J. Trophic link between syntrophic acetogens and homoacetogens during the anaerobic acidogenic fermentation of sewage sludge. *Biochem Eng J*. 2013; 70:1–8. <https://doi.org/10.1016/j.bej.2012.09.012>
32. Gilmore SP, Henske JK, Sexton JA, Solomon KV, Seppälä S, Yoo JI, et al. Genomic analysis of methanogenic archaea reveals a shift towards energy conservation. *BMC Genomics*. 2017; 18(1):639. <https://doi.org/10.1186/s12864-017-4036-4> PMID: 28826405
33. Hibbing ME, Fuqua C, Parsek MR, Peterson SB. Bacterial competition: surviving and thriving in the microbial jungle. *Nat Rev Microbiol*. 2010; 8(1):15–25. <https://doi.org/10.1038/nrmicro2259> PMID: 19946288
34. Sela-Adler M, Ronen Z, Herut B, Antler G, Vigderovich H, Eckert W, et al. Co-existence of Methanogenesis and Sulfate Reduction with Common Substrates in Sulfate-Rich Estuarine Sediments. *Front Microbiol*. 2017; 8:766. <https://doi.org/10.3389/fmicb.2017.00766> PMID: 28529500
35. Klüber HD, Conrad R. Effects of nitrate, nitrite, NO and N₂O on methanogenesis and other redox processes in anoxic rice field soil. *FEMS Microbiol Ecol*. 1998; 25(3):301–18. <https://doi.org/10.1111/j.1574-6941.1998.tb00482.x>
36. Garcia JL, Patel BK, Ollivier B. Taxonomic, phylogenetic, and ecological diversity of methanogenic Archaea. *Anaerobe*. 2000; 6(4):205–26. <https://doi.org/10.1006/anae.2000.0345> PMID: 16887666
37. Roden EE, Wetzel RG. Competition between Fe(III)-reducing and methanogenic bacteria for acetate in iron-rich freshwater sediments. *Microb Ecol*. 2003; 45(3):252–8. <https://doi.org/10.1007/s00248-002-1037-9> PMID: 12658519
38. Bodelier PLE, Steenbergh AK. Interactions between methane and the nitrogen cycle in light of climate change. *Current Opinion in Environmental Sustainability*. 2014; 9–10:26–36. <https://doi.org/10.1016/j.cosust.2014.07.004>
39. Boon PI, Mitchell A. Methanogenesis in the sediments of an Australian freshwater wetland: Comparison with aerobic decay, and factors controlling methanogenesis. *FEMS Microbiol Ecol*. 1995; 18(3):175–90. <https://doi.org/10.1111/j.1574-6941.1995.tb00175.x>
40. Oremland RS, Polcin S. Methanogenesis and sulfate reduction: competitive and noncompetitive substrates in estuarine sediments. *Appl Environ Microbiol*. 1982; 44(6):1270–6. <https://doi.org/10.1128/AEM.44.6.1270-1276.1982> PMID: 16346144
41. Purdy KJ, Munson MA, Nedwell DB, Martin Embley T. Comparison of the molecular diversity of the methanogenic community at the brackish and marine ends of a UK estuary. *FEMS Microbiol Ecol*. 2002; 39(1):17–21. <https://doi.org/10.1111/j.1574-6941.2002.tb00902.x> PMID: 19709180
42. Chen J, Wade MJ, Doling J, Soyer OS. Increasing sulfate levels show a differential impact on synthetic communities comprising different methanogens and a sulfate reducer. *J R Soc Interface*. 2019; 16(154):20190129. <https://doi.org/10.1098/rsif.2019.0129> PMID: 31064258
43. Hanson RS, Hanson TE. Methanotrophic bacteria. *Microbiol Rev*. 1996; 60(2):439–71. PMID: 8801441
44. Bowman J. The methanotrophs—the families Methylococcaceae and Methylocystaceae. *The Prokaryotes: Volume 5: Proteobacteria: Alpha and*. 2006.
45. Mohammadi SS, Pol A, van Alen T, Jetten MSM, Op den Camp HJM. Ammonia Oxidation and Nitrite Reduction in the Verrucomicrobial Methanotroph *Methylacidiphilum fumarolicum* SolV. *Front Microbiol*. 2017; 8:1901. <https://doi.org/10.3389/fmicb.2017.01901> PMID: 29021790
46. Waterhouse J, Brodie J, Lewis S, Mitchell A. Quantifying the sources of pollutants in the Great Barrier Reef catchments and the relative risk to reef ecosystems. *Mar Pollut Bull*. 2012; 65(4–9):394–406. <https://doi.org/10.1016/j.marpolbul.2011.09.031> PMID: 22070980
47. Kroon FJ, Kuhnert PM, Henderson BL, Wilkinson SN, Kinsey-Henderson A, Abbott B, et al. River loads of suspended solids, nitrogen, phosphorus and herbicides delivered to the Great Barrier Reef lagoon. *Mar Pollut Bull*. 2012; 65(4–9):167–81. <https://doi.org/10.1016/j.marpolbul.2011.10.018> PMID: 22154273
48. Maher DT, Santos IR, Leuven JRFW, Oakes JM, Eler DV, Carvalho MC, et al. Novel use of cavity ring-down spectroscopy to investigate aquatic carbon cycling from microbial to ecosystem scales. *Environ Sci Technol*. 2013; 47(22):12938–45. <https://doi.org/10.1021/es4027776> PMID: 24131451
49. Lalonde K, Middlestead P, Gélinas Y. Automation of ¹³C/¹²C ratio measurement for freshwater and seawater DOC using high temperature combustion. *Limnol Oceanogr Methods*. 2014; 12(12):816–29.
50. Eyre BD, Ferguson AJP. Benthic metabolism and nitrogen cycling in a sub-tropical east Australian estuary (Brunswick)—temporal variability and controlling factors. *Limnol Oceanogr*. 2005; 50(1):81.

51. Johnston GP, Leff LG. Bacterial community composition and biogeochemical heterogeneity in PAH-contaminated riverbank sediments. *J Soils Sediments*. 2015; 15(1):225–39. <https://doi.org/10.1007/s11368-014-1005-2>
52. Zhang J, Kobert K, Flouri T, Stamatakis A. PEAR: a fast and accurate Illumina Paired-End reAd mergeR. *Bioinformatics*. 2014; 30(5):614–20. <https://doi.org/10.1093/bioinformatics/btt593> PMID: 24142950
53. Caporaso JG, Kuczynski J, Stombaugh J, Bittinger K, Bushman FD, Costello EK, et al. QIIME allows analysis of high-throughput community sequencing data. *Nat Methods*. 2010; 7(5):335–6. <https://doi.org/10.1038/nmeth.f.303> PMID: 20383131
54. Edgar RC, Haas BJ, Clemente JC, Quince C, Knight R. UCHIME improves sensitivity and speed of chimera detection. *Bioinformatics*. 2011; 27(16):2194–200. <https://doi.org/10.1093/bioinformatics/btr381> PMID: 21700674
55. Edgar RC. UPARSE: highly accurate OTU sequences from microbial amplicon reads. *Nat Methods*. 2013; 10(10):996–8. <https://doi.org/10.1038/nmeth.2604> PMID: 23955772
56. DeSantis TZ, Hugenholtz P, Larsen N, Rojas M, Brodie EL, Keller K, et al. Greengenes, a chimera-checked 16S rRNA gene database and workbench compatible with ARB. *Appl Environ Microbiol*. 2006; 72(7):5069–72. <https://doi.org/10.1128/AEM.03006-05> PMID: 16820507
57. Huson DH, Beier S, Flade I, Górska A, El-Hadidi M, Mitra S, et al. MEGAN Community Edition—Interactive Exploration and Analysis of Large-Scale Microbiome Sequencing Data. *PLoS Comput Biol*. 2016; 12(6):e1004957. <https://doi.org/10.1371/journal.pcbi.1004957> PMID: 27327495
58. Glud RN. Oxygen dynamics of marine sediments. *Mar Biol Res*. 2008; 4(4):243–89. <https://doi.org/10.1080/17451000801888726>
59. Probandt D, Knittel K, Tegetmeyer HE, Ahmerkamp S, Holtappels M, Amann R. Permeability shapes bacterial communities in sublittoral surface sediments. *Environ Microbiol*. 2017; 19(4):1584–99. <https://doi.org/10.1111/1462-2920.13676> PMID: 28120371
60. Higashino M. Quantifying a significance of sediment particle size to hyporheic sedimentary oxygen demand with a permeable stream bed. *Environ Fluid Mech*. 2013; 13(3):227–41. <https://doi.org/10.1007/s10652-012-9262-3>
61. Borrel G, O'Toole PW, Harris HMB, Peyret P, Brugère J-F, Gribaldo S. Phylogenomic data support a seventh order of Methylophilic methanogens and provide insights into the evolution of Methanogenesis. *Genome Biol Evol*. 2013; 5(10):1769–80. <https://doi.org/10.1093/gbe/evt128> PMID: 23985970
62. Tas N, van Eekert MHA, Schraa G, Zhou J, de Vos WM, Smidt H. Tracking functional guilds: "Dehalococcoides" spp. in European river basins contaminated with hexachlorobenzene. *Appl Environ Microbiol*. 2009; 75(14):4696–704. <https://doi.org/10.1128/AEM.02829-08> PMID: 19376891
63. Taş N, van Eekert MHA, de Vos WM, Smidt H. The little bacteria that can—diversity, genomics and eco-physiology of 'Dehalococcoides' spp. in contaminated environments. *Microb Biotechnol*. 2010; 3(4):389–402. <https://doi.org/10.1111/j.1751-7915.2009.00147.x> PMID: 21255338
64. Torlapati J, Clement TP, Schaefer CE, Lee K-K. Modeling Dehalococcoides sp. Augmented Bioremediation in a Single Fracture System. *Ground Water Monit Remediat*. 2012; 32(3):75–83. <https://doi.org/10.1111/j.1745-6592.2011.01392.x>
65. Rissanen AJ, Karvinen A, Nykänen H, Peura S, Tirola M, Mäki A, et al. Effects of inorganic electron acceptors on methanogenesis and methanotrophy and on the community structure of bacteria and archaea in sediments of a boreal lake. 2016/4/12016. p. EPSC2016-3726.
66. Kim SY, Pramanik P, Bodelier PLE, Kim PJ. Cattle Manure Enhances Methanogens Diversity and Methane Emissions Compared to Swine Manure under Rice Paddy. *PLoS One*. 2014; 9(12):e113593. <https://doi.org/10.1371/journal.pone.0113593> PMID: 25494364
67. Takii S, Fukui M. Relative Importance of Methanogenesis, Sulfate Reduction and Denitrification in Sediments of the Lower Tama River. *Bulletin of Japanese Society of Microbial Ecology (日本微生物生態学会報)*. 1991; 6(1):9–17. <https://doi.org/10.1264/microbes1986.6.9>
68. Tong C, Cadillo-Quiroz H, Zeng ZH, She CX, Yang P, Huang JF. Changes of community structure and abundance of methanogens in soils along a freshwater–brackish water gradient in subtropical estuarine marshes. *Geoderma*. 2017; 299:101–10. <https://doi.org/10.1016/j.geoderma.2017.03.026>
69. Sachse A, Henrion R, Gelbrecht J, Steinberg CEW. Classification of dissolved organic carbon (DOC) in river systems: Influence of catchment characteristics and autochthonous processes. *Org Geochem*. 2005; 6(36):923–35. <https://doi.org/10.1016/j.orggeochem.2004.12.008>
70. Egger M, Lenstra W, Jong D, Meysman FJR, Sapart CJ, van der Veen C, et al. Rapid Sediment Accumulation Results in High Methane Effluxes from Coastal Sediments. *PLoS One*. 2016; 11(8):e0161609. <https://doi.org/10.1371/journal.pone.0161609> PMID: 27560511

71. Borrel G, Lehours A-C, Crouzet O, Jézéquel D, Rockne K, Kulczak A, et al. Stratification of Archaea in the deep sediments of a freshwater meromictic lake: vertical shift from methanogenic to uncultured archaeal lineages. *PLoS One*. 2012; 7(8):e43346. <https://doi.org/10.1371/journal.pone.0043346> PMID: 22927959
72. Purdy KJ, Munson MA, Cresswell-Maynard T, Nedwell DB, Embley TM. Use of 16S rRNA-targeted oligonucleotide probes to investigate function and phylogeny of sulphate-reducing bacteria and methanogenic archaea in a UK estuary. *FEMS Microbiol Ecol*. 2003; 44(3):361–71. [https://doi.org/10.1016/S0168-6496\(03\)00078-3](https://doi.org/10.1016/S0168-6496(03)00078-3) PMID: 19719617
73. Bai Y-N, Wang X-N, Wu J, Lu Y-Z, Fu L, Zhang F, et al. Humic substances as electron acceptors for anaerobic oxidation of methane driven by ANME-2d. *Water Res*. 2019; 164:114935. <https://doi.org/10.1016/j.watres.2019.114935> PMID: 31387057
74. Vignerot A, Cruaud P, Pignet P, Caprais J-C, Cambon-Bonavita M-A, Godfroy A, et al. Archaeal and anaerobic methane oxidizer communities in the Sonora Margin cold seeps, Guaymas Basin (Gulf of California). *ISME J*. 2013; 7(8):1595–608. <https://doi.org/10.1038/ismej.2013.18> PMID: 23446836
75. Wang F-P, Zhang Y, Chen Y, He Y, Qi J, Hinrichs K-U, et al. Methanotrophic archaea possessing diverging methane-oxidizing and electron-transporting pathways. *ISME J*. 2014; 8(5):1069–78. <https://doi.org/10.1038/ismej.2013.212> PMID: 24335827
76. Kristensen E, Holmer M, Bussarawit N. Benthic metabolism and sulfate reduction in a Southeast Asian mangrove swamp. 1991; 73:93–103. <https://doi.org/10.3354/meps073093>
77. Serrano-Silva N, Valenzuela-Encinas C, Marsch R, Dendooven L, Alcántara-Hernández RJ. Changes in methane oxidation activity and methanotrophic community composition in saline alkaline soils. *Extremophiles*. 2014; 18(3):561–71. <https://doi.org/10.1007/s00792-014-0641-1> PMID: 24638260
78. Pereira AD, Cabezas A, Etchebehere C, Chernicharo CA dL, de Araújo JC. Microbial communities in anammox reactors: a review. *Environmental Technology Reviews*. 2017; 6(1):74–93. <https://doi.org/10.1080/21622515.2017.1304457>
79. Fang Herbert HP, Zhou G-M. Interactions of Methanogens and Denitrifiers in Degradation of Phenols. *J Environ Eng*. 1999; 125(1):57–63. [https://doi.org/10.1061/\(ASCE\)0733-9372\(1999\)125:1\(57\)](https://doi.org/10.1061/(ASCE)0733-9372(1999)125:1(57)).
80. Gieseke A, Tarre S, Green M, de Beer D. Nitrification in a biofilm at low pH values: role of in situ micro-environments and acid tolerance. *Appl Environ Microbiol*. 2006; 72(6):4283–92. <https://doi.org/10.1128/AEM.00241-06> PMID: 16751543
81. Trampe ECL, Larsen JEN, Glaring MA, Stougaard P, Kühl M. In situ Dynamics of O₂, pH, Light, and Photosynthesis in Ikaite Tufa Columns (Ikka Fjord, Greenland)-A Unique Microbial Habitat. *Front Microbiol*. 2016; 7:722. <https://doi.org/10.3389/fmicb.2016.00722> PMID: 27242741
82. Tavormina PL, Ussler W 3rd, Joye SB, Harrison BK, Orphan VJ. Distributions of putative aerobic methanotrophs in diverse pelagic marine environments. *ISME J*. 2010; 4(5):700–10. <https://doi.org/10.1038/ismej.2009.155> PMID: 20147984
83. Sze MA, Schloss PD. The Impact of DNA Polymerase and Number of Rounds of Amplification in PCR on 16S rRNA Gene Sequence Data. *mSphere*. 2019; 4(3). <https://doi.org/10.1128/mSphere.00163-19> PMID: 31118299
84. Smith CJ, Osborn AM. Advantages and limitations of quantitative PCR (Q-PCR)-based approaches in microbial ecology. *FEMS Microbiol Ecol*. 2009; 67(1):6–20. <https://doi.org/10.1111/j.1574-6941.2008.00629.x> PMID: 19120456
85. Props R, Kerckhof F-M, Rubbens P, De Vrieze J, Hernandez Sanabria E, Waegeman W, et al. Absolute quantification of microbial taxon abundances. *ISME J*. 2017; 11(2):584–7. <https://doi.org/10.1038/ismej.2016.117> PMID: 27612291
86. Özel Duygan BD, Hadadi N, Babu AF, Seyfried M, van der Meer JR. Rapid detection of microbiota cell type diversity using machine-learned classification of flow cytometry data. *Commun Biol*. 2020; 3(1):379. <https://doi.org/10.1038/s42003-020-1106-y> PMID: 32669688
87. Adyasari D, Hassenrück C, Oehler T, Sabdaningsih A, Moosdorf N. Microbial community structure associated with submarine groundwater discharge in northern Java (Indonesia). *Sci Total Environ*. 2019; 689:590–601. <https://doi.org/10.1016/j.scitotenv.2019.06.193> PMID: 31279205
88. Mackey KRM, Hunter-Cevera K, Britten GL, Murphy LG, Sogin ML, Huber JA. Seasonal Succession and Spatial Patterns of Synechococcus Microdiversity in a Salt Marsh Estuary Revealed through 16S rRNA Gene Oligotyping. *Front Microbiol*. 2017; 8:1496. <https://doi.org/10.3389/fmicb.2017.01496> PMID: 28848514
89. Wasmund K, Mußmann M, Loy A. The life sulfuric: microbial ecology of sulfur cycling in marine sediments. *Environ Microbiol Rep*. 2017; 9(4):323–44. <https://doi.org/10.1111/1758-2229.12538> PMID: 28419734
90. Nelson MB, Martiny AC, Martiny JBH. Global biogeography of microbial nitrogen-cycling traits in soil. *Proc Natl Acad Sci U S A*. 2016; 113(29):8033–40. <https://doi.org/10.1073/pnas.1601070113> PMID: 27432978